NANO LETTERS

2006
Vol. 6, No. 7
1420−1424

Using Perylene-Doped Polymer Nanotubes as Fluorescence Sensors

Soohyun Lee, Astrid M. Müller, Rabih Al-Kaysi, and Christopher J. Bardeen*

Department of Chemistry, University of California, Riverside, California 92521

Received February 24, 2006; Revised Manuscript Received June 2, 2006

ABSTRACT

Al_2O_3 filters (200 nm) are used as templates to form polymer nanotubes containing an energy donor (perylene). The perylene is isolated from chemical interactions but can undergo electronic energy transfer to acceptor molecules in aqueous solutions passing through the membrane. This energy transfer is analyzed quantitatively in terms of both radiative and nonradiative (Forster transfer) mechanisms and provides a way for the chemically inert filter to sense the presence of analyte molecules in the filtrate.

Introduction. There is currently much interest in using nanostructured materials in sensing applications. The high surface-to-volume ratio inherent in nanoscale structures enhances the amount of material exposed to surface interactions with analyte molecules, which then modify some material property like fluorescence or conductivity. Recently, work in several groups has demonstrated the sensing capabilities of nanoporous materials, which can range from zeolites to filter membranes.[1−4] This approach combines the high surface-to-volume advantages of nanostructured materials with an architecture that is compatible with sample filtration and microfluidic separations.[5] In these cases, the analyte molecules interact chemically with the sensor molecules that line the interior of the pores. Nonspecific adsorption and release of the analyte are problems that must be overcome in each specific application. For some applications, it would be desirable to have a sensor that does not rely on chemically specific interactions between molecules. Such a structure would function as a passive filter, allowing the analyte solution to flow through unimpeded, while its walls could register the presence of an analyte without the need for adsorption or chemical reaction. To avoid chemical interactions between solution molecules and the sensor, the analyte−sensor interaction must rely on a through-space interaction. The best candidate for such a through-space interaction is electronic energy transfer (EET) resulting from the Coulombic interaction between two electronic transition dipole moments.

In this paper, we present a preliminary realization of a chemically inert sensor-filter that makes use of EET from a donor embedded in the pore walls to an acceptor dissolved in the analyte solution. The system we study is outlined schematically in Figure 1. The donor−acceptor system is comprised of perylene and disodium fluorescein (DSF). A

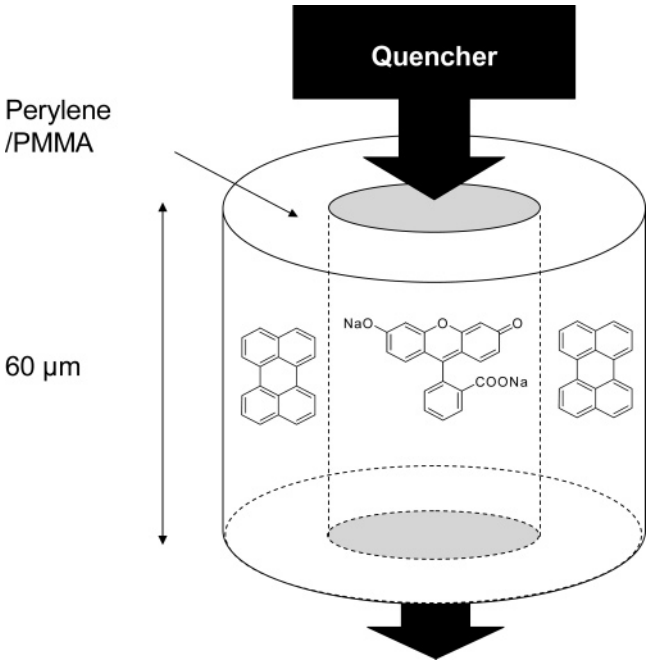

Figure 1. Schematic diagram of a perylene/PMMA nanotube with an aqueous solution of fluorescein traveling down the inner channel.

200 nm Al_2O_3 Anodisc filter is used as a template for the formation of polymethyl methacrylate (PMMA) nanotubes with an inner diameter of approximately 100 nm. We find that the fluorescence of perylene molecules dissolved in the PMMA is reversibly quenched by the presence of the DSF in aqueous solution that is forced through the filter. We analyze the decrease in the perylene fluorescence in terms of two mechanisms for EET. The first is reabsorption of the emitted perylene fluorescence by the DSF in the Anodisc pores, also known as the "inner filter effect". The second is Forster resonance energy transfer (FRET) from the perylene to the DSF across the PMMA−water interface. Both effects

* Corresponding author. E-mail: christopher.bardeen@ucr.edu.

10.1021/nl060446z CCC: $33.50 © 2006 American Chemical Society
Published on Web 06/21/2006

can be understood in terms of simple models. This work demonstrates how polymer nanotubes can be used as filters that sense the chemical composition of the filtrate without relying on surface adsorption or a chemical reaction between sensor and analyte.

Experimental Section. *Polymeric Nanotube Preparation.* Alumina membrane filters (Anodisc; Whatman) with 200-nm-diameter pores and 60 μm thickness were used as templates to make uniform nanotubes.[6] Measured amounts of perylene (Aldrich, 99%) and PMMA (Aldrich) were dissolved in acetone (Fisher Scientific, spectral grade). Nanotubes were prepared by vacuum filtering a 4.22% PMMA/acetone (w/w) solution with 4.7 mM or 0.1070 M perylene/PMMA concentration into the pores of the template membrane. The polymer solution (100 μL) was placed on the top of the membrane, and a house vacuum was applied to the other side of the membrane. The vacuum was applied until the entire volume of the solution was pulled through the membrane and the solvent evaporated. After the solvent had evaporated, water was filtered through the membrane to make sure that open-ended tubes had been obtained. The flow rate through the Anodisc membranes containing the PMMA tubes was approximately 30−50% of the rate through the bare Anodisc filter.

Fluorescence Measurements. A drop of DSF (Exiton Chemical) solution in water (Millipore Q) placed on the nanotube Anodisc was quickly absorbed into the membrane, which was then tightly sandwiched between glass coverslips, squeezing out excess dye solution. Care was taken so that the Anodisc sample did not dry out during the measurements. Steady-state fluorescence spectra were measured using front face excitation in a Jobin-Yvon-Spex Fluorolog Tau-3 fluorescence spectrophotometer. The excitation wavelength was 400 nm. Fluorescence lifetimes were measured by exciting the same samples at normal incidence to the membrane surface using femtosecond pulses centered at 400 nm and collecting the emission at 15°. The fluorescence was focused into a spectrometer (Spectra Pro-150) with a 150 grooves/mm grating to disperse the spectrum before it entered a picosecond time-resolved streak camera (Hamamatsu streak scope C4334). The time resolution of the streak camera was 15 ps, and the spectral resolution was 2 nm. Ten-thousand scans taken over the course of ~5 min were required to obtain the measured fluorescence lifetimes with <3% variation on a given sample.

Scanning Electron Microscopy (SEM). An alumina membrane containing the nanotubes was attached onto Cu-foil tape (3M) to provide a conductive support. It was then immersed in a 2 M NaOH solution for 1 h to dissolve the alumina and thoroughly rinsed with distilled water to remove the dissolved alumina and NaOH. This left the surface with polymeric nanotubes protruding like the bristles of a brush, as seen in Figure 2. The average outer diameter of the tubes is 200 nm, as expected based on the Anodisc pore size. After vacuum-drying for 15 min, it was affixed onto the SEM sample holder with carbon tape and sputter coated with gold/palladium (alloy mixed in 2:3 ratio) using a Cressington sputter coater for 40 s. SEM images were obtained using

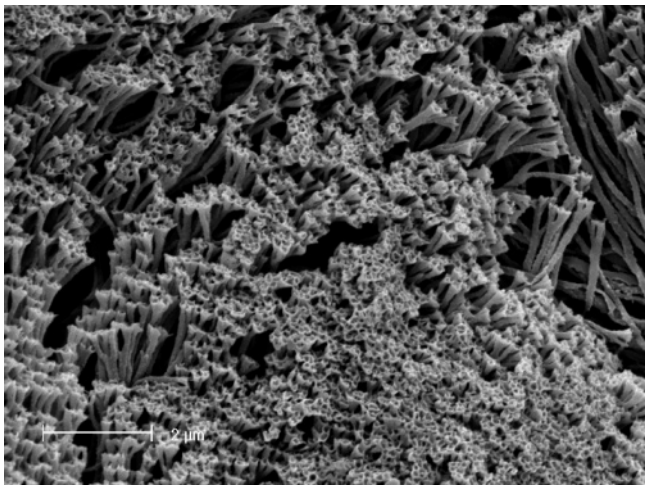

Figure 2. SEM image of nanotubes made from a 4.22% PMMA/acetone solution using a 200 nm Anodisc membrane as a template. The Anodisc membrane has been dissolved away, leaving only the polymer nanotubes.

FEI XL 30-FEG at the voltage of 5.0 kV. A semiquantitative composition analysis of the SEM image yielded only peaks due to carbon and oxygen and the sputter coating, with no sign of residual aluminum.

Results and Discussion. Figure 2 shows an SEM image of the polymer nanotubes. They are open-ended, and an analysis of the image yields an inner diameter of about 100 nm with about a 25% variation. The perylene dissolved in the PMMA tubes appears to be completely shielded from external chemical interactions: its fluorescence spectrum and lifetime are identical to those of perylene in a neat PMMA film on a glass substrate. When the Anodisc is saturated with a concentrated aqueous solution of Ag^+, which is known to form an exciplex with perylene,[7] or with triethylamine, which quenches perylene fluorescence via an electron-transfer reaction,[8] no effect on the nanotube perylene fluorescence is observed. These observations demonstrate that the perylene molecules are buried in the PMMA walls and have little or no physical contact with either the Al_2O_3 template material or the aqueous solution inside the tube. Thus, the perylene can only interact with analyte molecules via through-space mechanisms such as EET.

The absorption spectrum of DSF, a water soluble fluorescent dye, overlaps very well with the perylene emission, indicating that it would be a good energy acceptor. We can determine the Forster radius, R_0, using the equation

$$R_0^6 = \frac{9000 \ln(10)\, \phi_{fl} \kappa^2}{128 \pi^5 N_A n^4} \int \epsilon(\nu)\, f(\nu)\, \frac{d\nu}{\nu^4} \qquad (1)$$

where n is the index of refraction (1.33), ϕ_{fl} is the quantum yield of the donor (0.94 for perylene), κ^2 is an orientation factor (2/3 in a rotationally averaged solution), N_A is Avogadro's number, $\epsilon(\nu)$ is the DSF absorption spectrum, and $f(\nu)$ is the perylene fluorescence spectrum whose integral has been normalized to unity. The integral in eq 1 was evaluated between 423 and 526 nm. Using these parameters,

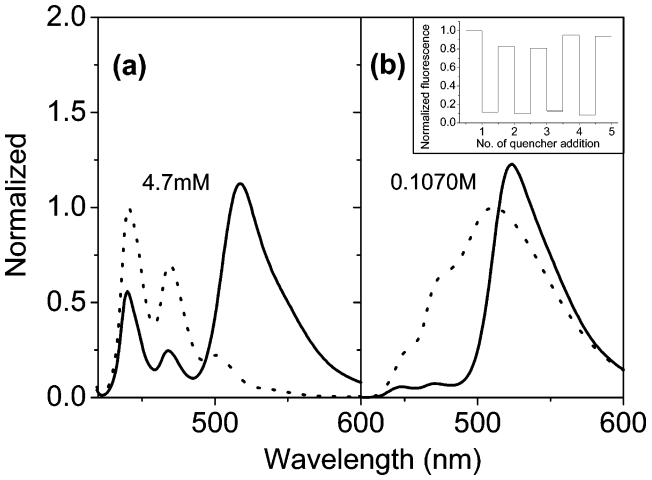

Figure 3. Comparison of fluorescence quenching of polymer nanotubes by a 1.9 mM DSF solution with perylene concentrations of (a) 4.7 mM and (b) 0.1070 M. Dotted lines are before a quencher is added, and solid lines are after the quencher is added. The inset of b shows the fluorescence intensity changes monitored at 473 nm through four cycles of addition and rinsing of the DSF solution.

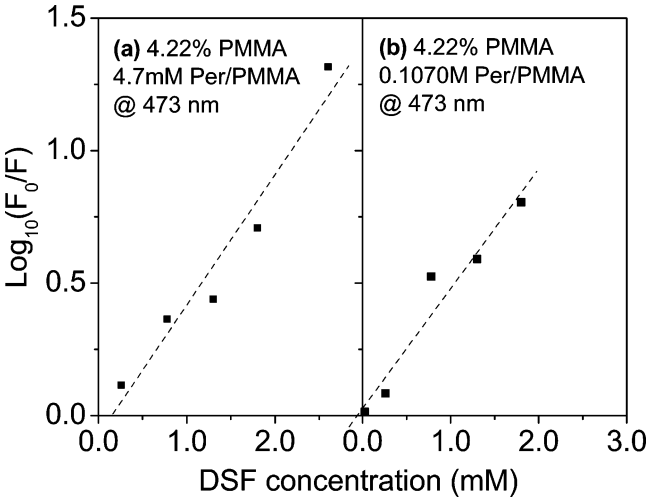

Figure 4. (a) Plot of the fluorescence quenching (fluorescence at 473 nm with and without the DSF solution) versus DSF concentration for the dilute 4.7 mM perylene/PMMA tubes. (b) Plot of the fluorescence quenching versus DSF concentration for the concentrated 107 mM perylene/PMMA tubes. Dashed lines show fits to the data using eq 2 in the text.

we obtain a Forster radius $R_0 = 5.9$ nm. When a 1.9 mM solution of DSF is allowed to saturate the Anodisc whose PMMA tubes are doped with 4.7 mM perylene, there is ~50% quenching of the steady-state perylene fluorescence accompanied by the appearance of an intense DSF emission, as shown in Figure 3a. We reasoned that the unquenched perylene emission originated from molecules located at large distances from the PMMA−water interface. By increasing the perylene concentration, we hoped that energy transfer between perylenes would allow such excitations to diffuse to the interface and be quenched as well. The results for 107 mM perylene/PMMA tubes are shown in Figure 3b. As expected, the quenching of the perylene fluorescence is more complete, but there is the added complication that the perylene emission is now dominated by the excimer species that forms at high concentrations.[9,10] For both perylene concentrations, the quenching effect is reversible, and the filter can be cycled multiple times, as illustrated in the inset to Figure 3b. Thus, from the standpoint of steady-state fluorescence detection, the PMMA nanotubes provide a robust way to detect DSF in solution.

We now turn our attention to the mechanism of the reversible fluorescence quenching. EET can occur via two different mechanisms. One way that an absorber can inhibit donor emission is by direct absorption of the emitted photons before they can escape the sample and travel to the detector. This is also known as radiative energy transfer or the inner filter effect and has been used for optical sensing.[11−13] Fluorescence reabsorption in a scattering medium is a complex problem[14,15] but in general should obey the Beer−Lambert law.[16] In this case F_{obs}, the observed fluorescence, is actually

$$F_{obs}(C) = F10^{-\epsilon CL} \qquad (2)$$

where F is the fluorescence emitted locally, ϵ and L are effective absorption coefficients and path lengths whose product ϵL determines the concentration dependence of the radiative quenching. Equation 2 predicts a linear increase in $\log[F_{obs}(0)/F_{obs}(C)]$ versus the DSF concentration, C, as observed in Figure 4 for both dilute and concentrated perylene tubes. We note that a traditional Stern−Volmer plot of the quenching data did not result in a linear curve. Using eq 2 to fit the data in Figure 4, we find an ϵL value of 490 for the 4.7 mM perylene tubes and 450 for the 107 mM perylene tubes. Given a peak ϵ of 10^5 $M^{-1}cm^{-1}$ for DSF, an average path length, L, for the escaping photons of 45−50 μm is obtained. These values for L are only approximate, because they depend on experimental factors such as scattering in the Anodisc and the angle of detection, but are reasonable given the 60 μm thickness of the Anodisc membrane.

Although the inner filter effect clearly plays a dominant role in the fluorescence quenching, nonradiative FRET also has a measurable effect. To isolate the effect of nonradiative EET quenching due to Forster transfer, one must measure the time-resolved fluorescence decay: nonradiative EET shortens the fluorescence lifetime, while radiative transfer leaves the donor lifetime unchanged.[17] In Figure 5a, we see that the addition of the DSF solution to the 4.7 mM perylene-doped tubes decreases the perylene fluorescence lifetime from 4.67 to 3.69 ns, or by about 20%. This change is well above the measurement error but does not equal the 50% quenching deduced from the steady-state fluorescence, indicating that the quenching of the steady-state fluorescence is due mostly to radiative transfer, as assumed in the preceding paragraph. We obtain similar results for the 107 mM perylene-doped tubes (Figure 5b), where the decays are now biexponential and where the average lifetime changes from 1.68 to 1.13 ns. This 30% decrease again does not equal the ~90% decrease observed in the steady-state data. The greater decrease in the more concentrated perylene-doped

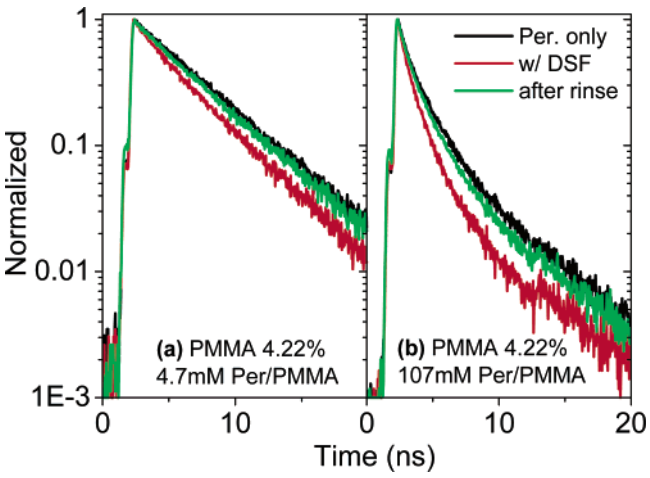

Figure 5. Fluorescence lifetime data for (a) 4.7 mM perylene nanotubes and (b) 107 mM perylene nanotubes. Black, before addition of 1.8 mM DSF solution; red, after addition of 1.8 mM DSF solution; green, after rinsing DSF solution away using distilled water.

tubes is likely due to slightly better overlap of the excimer emission with the DSF absorption. Finally, we note that the fluorescence decays recover to within 10% of their original values after the DSF is rinsed away, showing that both the radiative and nonradiative quenching processes are reversible.

The advantage of using the nonradiative quenching component as a sensing motif is that it depends only on the nanometer scale tube geometry rather than the scattering properties of the macroscopic sample. There are relatively few experimental examples of photoinduced interactions between molecules across a polymer−solvent interface,[18−20] and we could find only one reported instance of interfacial EET.[21] Fortunately, Winnik and co-workers have provided a theoretical framework that can be used to analyze such systems.[22,23] The fluorescence decay, $I_D(t)$, of the donor is given by

$$I_D(t) = I_D(0)e^{-t/\tau_D}\int_{R_1}^{R_2} dR_D \phi(R_D,t)\, C(R_D) \qquad (3)$$

where $C(R_D)$ is the concentration of donors in a hollow cylinder of inner radius R_1 and outer radius R_2, τ_D is the donor lifetime in the absence of EET, and the time-dependent energy transfer probability $\phi(R_D,t)$ is obtained from the equation

$$\frac{-\ln(\phi(R_D,t))}{4} = \int_0^\infty dz \int_0^{R_1} C_A R_A\, dR_A \int_0^\pi d\theta \left[1 - \exp\left[-\frac{3\kappa^2}{2\tau_D}\frac{R_0^6 t}{(R_D^2 + R_A^2 + z^2 - 2R_D R_A \cos(\theta))^3}\right]\right] \qquad (4)$$

In this equation, κ^2 is the usual orientation factor found in the Forster equation, which is set to 2/3, and R_0 is the Forster radius. To obtain the simplified expression in eq 3, we have assumed that the volume occupied by the donor and acceptor molecules is negligible. Using eq 4 and the values $R_0 = 5.9$ nm, $\tau_D = 4.7$ ns, $R_1 = 50$ nm, and $R_2 = 100$ nm (corresponding to the 200 nm outer diameter of the tubes), we obtain an exponential decay for the quenched perylene donor fluorescence of 4.1 ns for the 4.7 mM perylene-doped tubes. It is not straightforward to use eq 4 to analyze donor quenching in the 107 mM perylene-doped tubes, where EET between donors plays a role and the spectral properties of the perylene excimer must be taken into account. The value for the 4.7 mM tubes is slightly longer than the experimentally observed decay time of 3.7 ns. If we increase R_1 to 70 nm, which makes the tube walls thinner and allows a greater fraction of the embedded perylene to undergo EET, then we calculate a decay time of 3.6 ns, in good agreement with the experimental value. It is possible that a radius value of $R_1 = 70$ nm is closer to the true average inner radius of the tubes than the $R_1 = 50$ nm estimated from the SEM images. From Figure 2, the ends of the tubes tend to swell, and it is also possible that the radius changes along the interior of the tube. Despite these possible complications, the simple theory works surprisingly well in describing the Forster quenching of the donor fluorescence in the tubes with no adjustable parameters.

Conclusions. This work has demonstrated that dye-doped PMMA nanotubes can be used as fluorescence sensors by virtue of their reversible quenching by concentrated aqueous solutions of DSF. This quenching is the result of two different mechanisms. The first involves direct reabsorption of the scattered perylene fluorescent photons by the DSF in the Anodisc, and depends on experimental details such as sample thickness and its scattering properties. The second mechanism involves interfacial EET on a nanometer length scale and is described well by theoretical calculations based on Forster transfer in a cylindrical geometry. In practice, the second mechanism could probably be made dominant by using thinner membranes to reduce the effective path length for reabsorption. Although the current paper represents a proof-of-principle demonstration, eventually the question of the practical sensitivity of the interfacial FRET detection will have to be addressed. Ultimately, one would want a system where the fluorescence lifetime shows a linear, Stern−Volmer type of dependence on analyte concentration. The modest (20%) change in fluorescence lifetime observed here requires a relatively high concentration of analyte. To increase the degree of quenching, and thus the sensitivity, we can take several approaches. First, we can make the nanotube walls thinner, so that a greater fraction of the donor molecules can undergo EET to acceptors in the channel. Second, we can use donor−donor EET to increase the number of donors that can be quenched by a single acceptor. In this context, conjugated polymers are more promising than dye-doped PMMA because of their enhanced EET properties.[24] Other types of matrixes may also be used instead of PMMA.[25] Although the present work represents a preliminary demonstration of the feasibility of nanotube fluorescence sensors, it seems likely that this type of structure can be exploited in a variety of ways to create chemically inert, high-throughput sensors.

Acknowledgment. This work was supported by NSF Grant CHE-0517095.

References

(1) Dai, J.; Baker, G. L.; Bruening, M. L. *Anal. Chem.* **2006**, *78*, 135−140.
(2) Wernette, D. P.; Swearingen, C. B.; Cropek, D. M.; Lu, Y.; Sweedler, J. V.; Bohn, P. W. *Analyst* **2006**, *131*, 41−47.
(3) Meinershagen, J. L.; Bein, T. *J. Am. Chem. Soc.* **1999**, *121*, 448−449.
(4) Kang, M.; Trofin, L.; Mota, M. O.; Martin, C. R. *Anal. Chem.* **2005**, *77*, 6243−6249.
(5) Kohli, P.; Wirtz, M.; Martin, C. R. *Electroanalysis* **2004**, *16*, 9−18.
(6) Cepak, V. M.; Martin, C. R. *Chem. Mater.* **1999**, *11*, 1363−1367.
(7) Dreeskamp, H.; Laufer, A. *Chem. Phys. Lett.* **1984**, *112*, 479−482.
(8) Inada, T. N.; Kikuchi, K.; Takahashi, Y.; Ikeda, H.; Miyashi, T. *J. Photochem. Photobiol., A* **2000**, *137*, 93−97.
(9) Ferreira, J. A.; Porter, G. *J. Chem. Soc., Faraday Trans. 2* **1977**, *73*, 340−348.
(10) Salamon, Z.; Bassler, H. *Chem. Phys.* **1985**, *100*, 393−400.
(11) He, H.; Li, H.; Mohr, G.; Kovacs, B.; Werner, T.; Wolfbeis, O. S. *Anal. Chem.* **1993**, *65*, 123−127.
(12) Shao, N.; Zhang, Y.; Cheung, S.; Yang, R.; Chan, W.; Mo, T.; Li, K.; Liu, F. *Anal. Chem.* **2005**, *77*, 7294−7303.
(13) Gabor, G.; Walt, D. R. *Anal. Chem.* **1991**, *63*, 793−796.
(14) Mammel, U.; Brun, M.; Oelkrug, D. *Fresenius' J. Anal. Chem.* **1992**, *344*, 147−152.
(15) Conte, J. C.; Martinho, J. M. G. *J. Lumin.* **1981**, *22*, 273−284.
(16) Kubista, M.; Sjoback, R.; Eriksson, S.; Albinsson, B. *Analyst* **1994**, *119*, 417−419.
(17) Birks, J. B. *Photophysics of Aromatic Molecules*; Wiley & Sons: London, 1970.
(18) Bergbreiter, D. E.; Gray, H. N.; Srinivas, B. *Macromolecules* **1994**, *27*, 7294−7301.
(19) Rolinski, O. J.; Birch, D. J. S. *Meas. Sci. Technol.* **1999**, *10*, 127−136.
(20) Tazuke, S.; Takasaki, R. *J. Polym. Sci.* **1983**, *21*, 1517−1527.
(21) Birch, D. J. S.; Holmes, A. S.; Darbyshire, M. *Meas. Sci. Technol.* **1995**, *6*, 243−247.
(22) Yekta, A.; Duhamel, J.; Winnik, M. A. *Chem. Phys. Lett.* **1995**, *235*, 119−125.
(23) Farinha, J. P. S.; Spiro, J. G.; Winnik, M. A. *J. Phys. Chem. B* **2004**, *108*, 16392−16400.
(24) McQuade, D. T.; Pullen, A. E.; Swager, T. M. *Chem. Rev.* **2000**, *100*, 2537−2574.
(25) Han, W. S.; Kang, Y.; Lee, S. J.; Lee, H.; Do, Y.; Lee, Y.-A.; Jung, J. H. *J. Phys. Chem. B* **2005**, *109*, 20661−20664.

NL060446Z